catalysts

MDPI

*Supplementary Materials*

# Mesoporous Methyl-Functionalized Titanosilicate Produced by Aerosol Process for the Catalytic Epoxidation of Olefins

**Lucia E. Manangon-Perugachi [1,3], Valentin Smeets [1], Alvise Vivian [2], Itika Kainthla [1], Pierre Eloy [1], Carmela Aprile [2], Damien P. Debecker [1] and Eric M. Gaigneaux [1,*]**

[1] Institute of Condensed Matter and Nanosciences (IMCN), Université catholique de Louvain (UCLouvain), Place Louis Pasteur 1, P.O. box L4.01.09, 1348 Louvain-la-Neuve, Belgium; lucia.manangon@epn.edu.ec (L.E.M.-P.); valentin.smeets@uclouvain.be (V.S.); itika.kainthla@uclouvain.be (I.K.); pierre.eloy@uclouvain.be (P.E.); damien.debecker@uclouvain.be (D.P.D.)
[2] Unit of Nanomaterial Chemistry, Department of Chemistry, University of Namur, 5000 Namur, Belgium; alvise.vivian@unamur.be (A.V.); carmela.aprile@unamur.be (C.A.)
[3] Department of Extractive Metallurgy, Escuela Politécnica Nacional, Quito 170517, Ecuador;
* Correspondence: eric.gaigneaux@uclouvain.be

**Content:**



**Citation:** Manangon-Perugachi, L.E.; Smeets, V.; Vivian, A.; Kainthla, I.; Eloy, P.; Aprile, C.; Debecker, D.P.; Gaigneaux, E.M. Mesoporous methyl-functionalized titanosilicate produced by aerosol process for the catalytic epoxidation of olefins. *Catalysts* **2021**, *11*, 196. https://doi.org/10.3390/catal11020196

Academic Editor: Consuelo Alvarez-Galvan
Received: 13 January 2021
Accepted: 28 January 2021
Published: 2 February 2021

**Publisher's Note:** MDPI stays neutral with regard to jurisdictional claims in published maps and institutional affiliations.

**Copyright:** © 2021 by the authors. Licensee MDPI, Basel, Switzerland. This article is an open access article distributed under the terms and conditions of the Creative Commons Attribution (CC BY) license (http://creativecommons.org/licenses/by/4.0/).

**Assessing the methylation degree by quantitative direct excitation solid-state $^{29}$Si MAS NMR investigation**

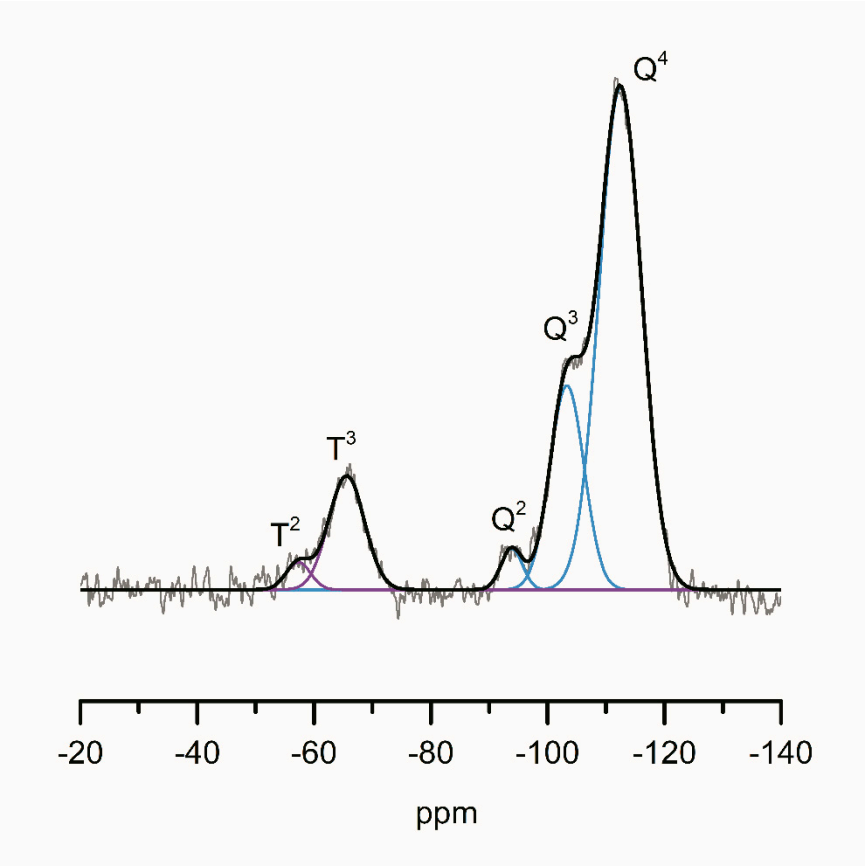


**Figure S1.** Deconvolution analysis using Gaussian functions on TS_Aer-14%Me to assign the chemical shift of the different contributions (i.e., $Q^4$, $Q^3$, $Q^2$…).

**Selection of the calcination temperature**

In this work, a mild calcination temperature of 623 K was selected to remove the templating agents while preserving the methyl-functionalization. Previous works successfully removed templating agents such as Pluronics at calcination temperatures lower than 823 K from silicalites [1,2]. Inspired by these works, the sample with a nominal MTES molar ratio of 0.20 was calcined at 523, 623, and 723 K in order to select the best calcination temperature. At 523 K, the incomplete removal of the templating agents was noticed based on the brown color of the sample (see Table S1). At higher calcination temperatures, the sample color was beige, suggesting that the removal of the templating agents improved. At this point, the selection of the calcination temperature was based on the difference in the preservation of the methyl-functionalization. This was determined by following the band corresponding to υ(Si–C) at 1279 $cm^{-1}$ by FTIR-ATR. As depicted in Figure S2, almost all the methyl moieties were lost due to calcination at 723 K, and good preservation of the methyl-functionalization was achieved at 623 K. Therefore, the calcination temperature selected for all the samples was 623 K.

**Table S1.** Ti-$SiO_2$ sample with MTES molar ratio of 0.20 calcined at 523, 623, and 723 K.

| Calcination temperature | | |
|---|---|---|
| 523 K | 623 K | 723 K |
|  |  | 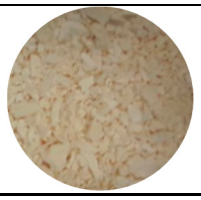 |

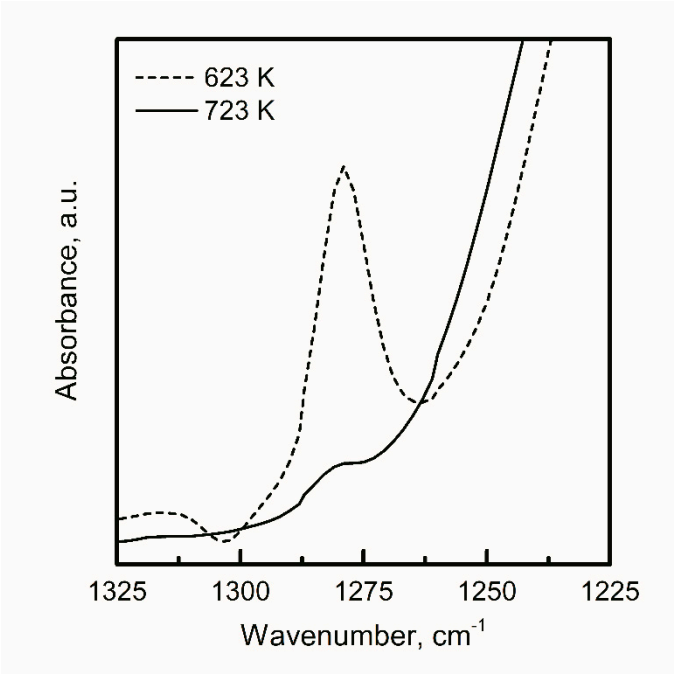


**Figure S2.** FTIR-ATR spectra of the sample with nominal MTES molar ratio of 0.20 calcined at 623 and 723 K in static air.

**T-plots derived from the $N_2$ adsorption branch of the isotherms of the TS_Aer-x%Me catalysts**

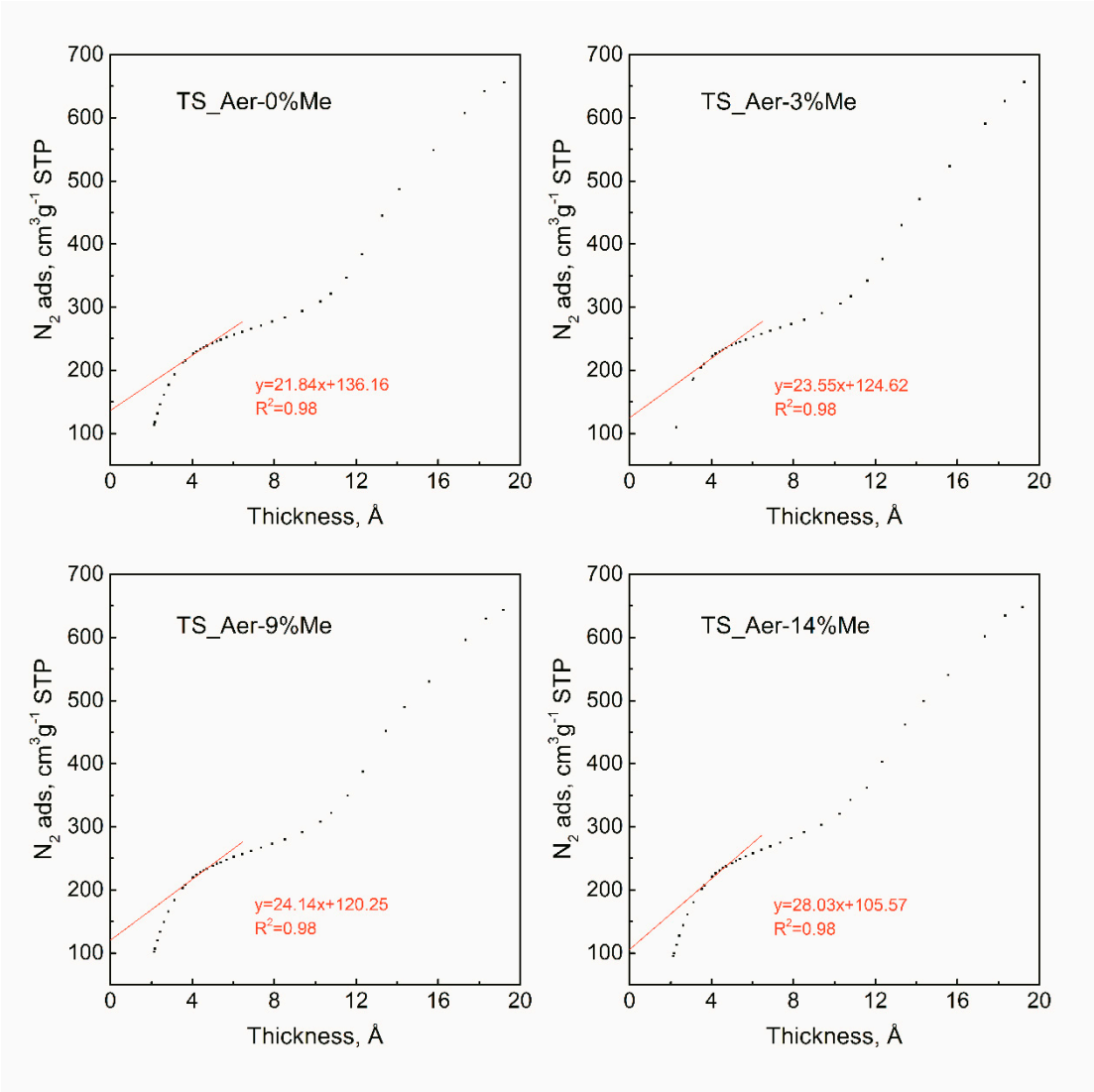


**Figure S3.** T-plots constructed based on the $N_2$ adsorption data for the TS_Aer-x%Me catalysts.

### Scanning electron microscopy images of TS_Aer-0%Me and TS_Aer-9%Me

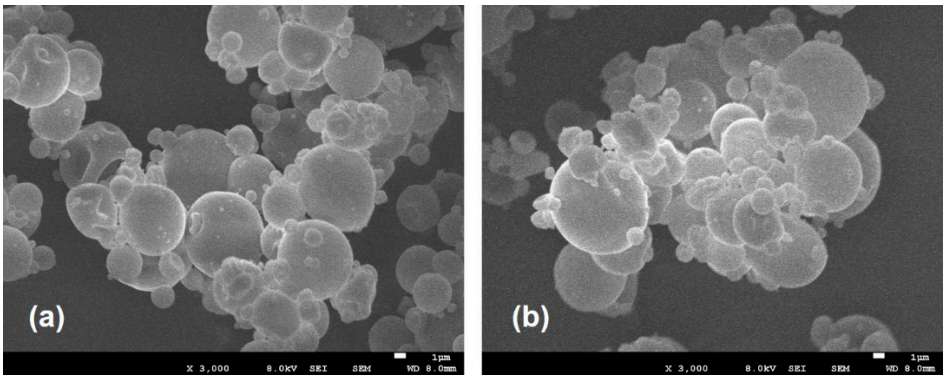


**Figure S4.** SEM images of TS_Aer-0%Me (**a**) and TS_Aer-9%Me (**b**).

### Vapor-phase water sorption experiments at 295 K for TS_Aer-0%Me, TS_Aer -9%Me, and TS_Aer -14%Me

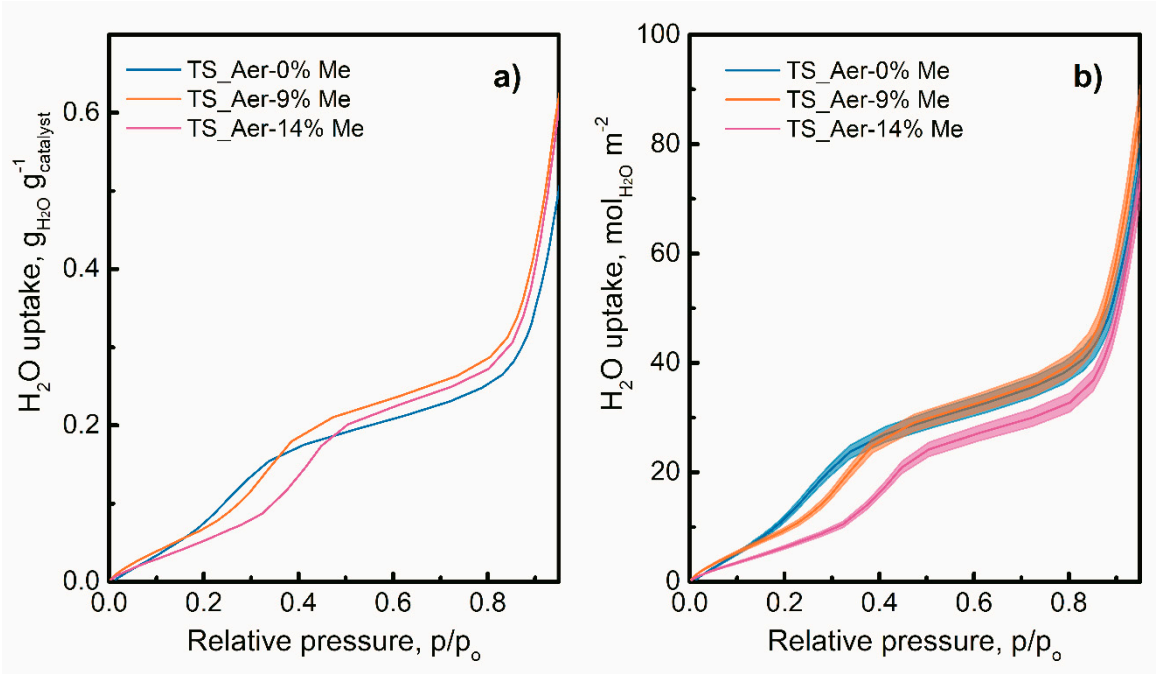


**Figure S5.** Water vapor adsorption isotherms for TS_Aer-0%Me, TS_Aer-9%Me, and TS_Aer-14%Me at 295 K. **a**) Water uptake in grams of water per gram of catalyst. **b**) For comparison among samples, the water uptake was normalized by the specific surface area corrected ($SSA_{corrected}$). The normalized water uptake values are depicted on the curve and the shaded regions denote the estimated uncertainty (5%) due to the $N_2$ physisorption measurement.

**Calculation of the band gap energy values (Eg) by the determination of the optical absorption edge for the TS_Aer-x%Me catalysts**

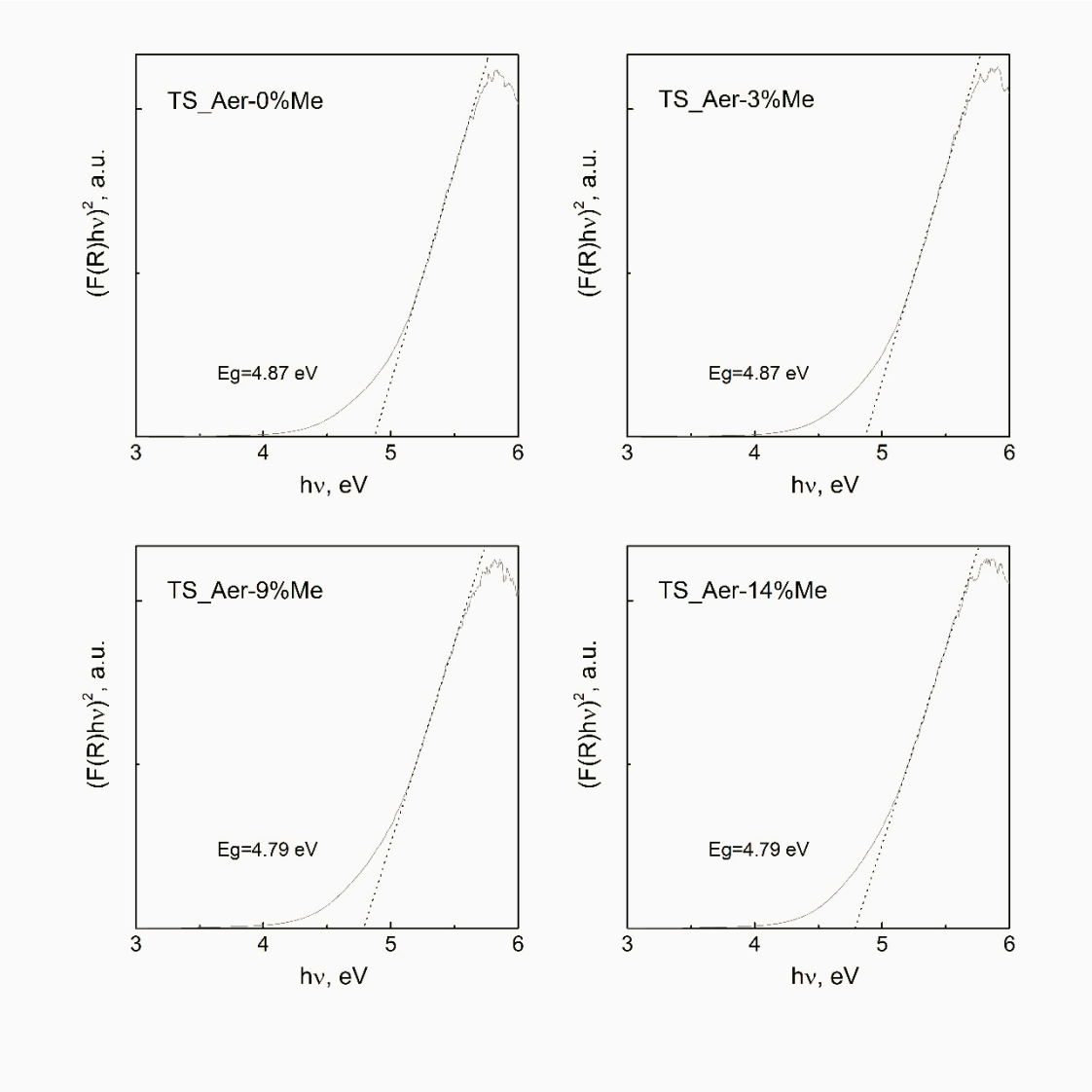


**Figure S6.** Eg calculation from the optical absorption edge in the DRUV spectra for the TS_Aer-x%Me catalysts using the Tauc method.

**Calculation of the band gap energy values (Eg) by the determination of the optical absorption edge for pristine and methyl-functionalized Ti-$SiO_2$ catalysts synthesized by conventional sol–gel method in a previous work**

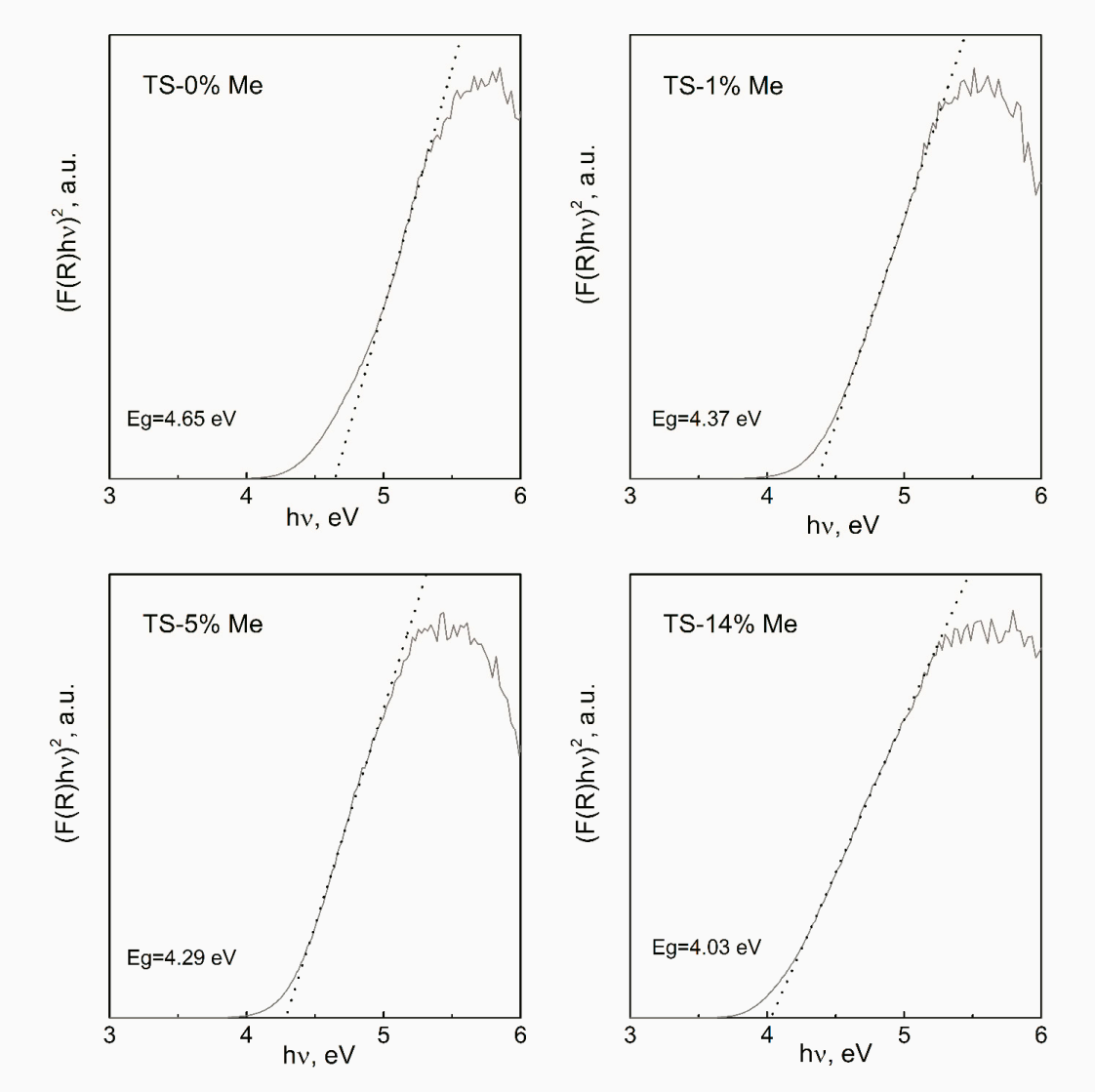


**Figure S7.** Eg calculation from the optical absorption edge in the DRUV spectra for pristine and methyl-functionalized Ti-$SiO_2$ catalysts synthesized by conventional sol–gel method [3] using the Tauc method.

**Description of the peak decomposition of Ti 2p XPS spectra for the samples TS_Aer-x%Me**

In this work, the shift and peak broadening of Ti 2p XPS spectra of the samples TS_Aer-x%Me compared to the spectrum of pure titanium dioxide ($TiO_2$) are attributed to the presence of FW-Ti together with EFW-Ti [4–9]. The quantification of these two Ti species was performed after some decomposition trials.

The first decomposition trial was performed under the following constraints: i) the spectrum is formed by two components which are FW-Ti and EFW-Ti, ii) the separation of Ti 2p $_{3/2}$ and Ti 2p $_{1/2}$ for each component is 5.7 eV [10], and iii) the area of Ti 2p $_{1/2}$ corresponds to half of the area of Ti 2p $_{3/2}$. This attempt showed that the binding energy of the FW-Ti 2p $_{3/2}$ component falls at 460.0-460.1 eV, which is in agreement with the literature [4,5,7,9]. On the other hand, the binding energy of the EFW-Ti 2p $_{3/2}$ component falls at 458.0-458.5, showing different binding energy values for the same component in each sample. This difference does not allow comparison of the quantification of FW-Ti and EFW-Ti species among the samples, so another constraint was added to set the difference of the two components as constant in all the samples. This value was selected based on the difference in binding energies of FW-Ti and EFW-Ti found in the literature, which is 1.5 eV [7,11,12]. Thus, the described constraint was included to perform the decomposition and quantification for all the samples.

**XPS surface elemental quantification of the TS_Aer-x%Me catalysts**

Table S2 shows the surface elemental quantification obtained from the XPS spectra for each sample.

**Table S2.** XPS surface elemental quantification.

| Sample | C (of which C–H) at.% | O at.% | Ti (of which FW-Ti) at.% | Si at.% |
|---|---|---|---|---|
| TS_Aer-0%Me | 5.1 (3.0) | 72.2 | 0.34 (0.29) | 22.3 |
| TS_Aer-3%Me | 6.3 (4.2) | 71.4 | 0.36 (0.30) | 21.9 |
| TS_Aer-9%Me | 7.0 (4.7) | 69.9 | 0.40 (0.32) | 22.6 |
| TS_Aer-14%Me | 8.5 (6.0) | 69.3 | 0.41 (0.32) | 21.8 |

**Calculation of Ti surface density on the catalysts TS_Aer-x%Me**

An example of the calculation of Ti surface density was performed for the sample TS_Aer-14%Me. The same calculation was performed for all the samples for the estimation of the Ti and FW-Ti surface density.

$$Ti\ surface\ density = \frac{0.019\ mol\ Ti}{mol\ (Si+Ti)} \cdot \frac{0.015\ mol\ (Si+Ti)}{g_{catalyst}} \cdot \frac{g_{catalyst}}{462\ m^2} \cdot \frac{6.022E23\ atoms\ Ti}{mol\ Ti} \cdot \frac{m^2}{1E18\ nm^2} = \frac{0.37\ atoms\ Ti}{nm^2} \quad (1)$$

Where

$\frac{0.019\ mol\ Ti}{mol\ (Si+Ti)}$ was determined from XPS analysis (Table 3);

$\frac{0.015\ mol\ (Si+Ti)}{g_{catalyst}}$ was determined from ICP-MS analysis;

$\frac{g_{catalyst}}{462\ m^2}$ is the inverse of the $SSA_{corrected}$ for the sample TS_Aer-14%Me;

$\frac{6.022E23\ atoms\ Ti}{mol\ Ti}$ is the Avogadro number.

**TBHP conversions of the TS_Aer-x%Me catalysts**

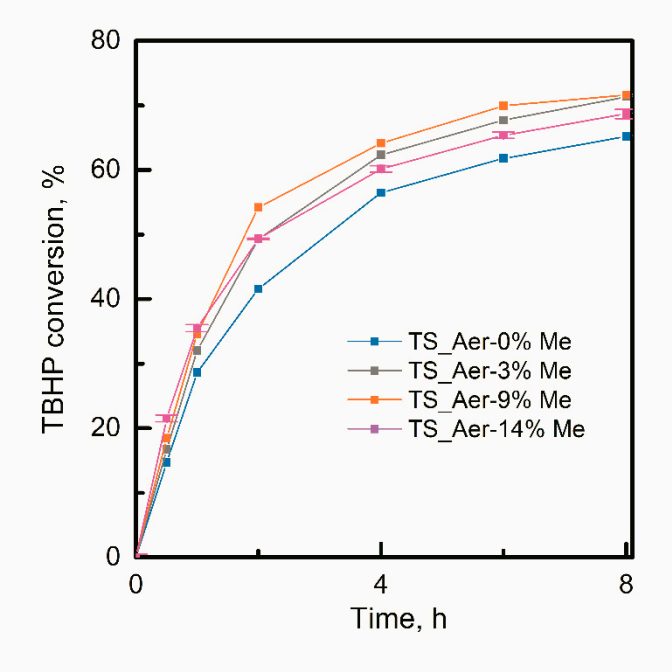


**Figure S8.** TBHP conversion as a function of reaction time of the TS_Aer-x%Me catalysts. Error bars are shown for TS_Aer-14%Me.

**Calculation of the Turnover Frequency values (TOF) for the TS_Aer-x%Me catalysts**

An example of the calculation of Turnover Frequency values (TOF) was performed for the sample TS_Aer-14%Me. The same calculation was performed for the rest of the samples.

$$TOF = \frac{\frac{0.0118\ mol_{TBHP}}{h\ g_{catalyst}}}{\frac{0.014\ mol\ FW - Ti}{mol\ (Si + Ti)} \cdot \frac{0.015\ mol\ (Si + Ti)}{g_{catalyst}}} = 57\ h^{-1} \quad (2)$$

Where

$\frac{0.0118\ mol_{TBHP}}{h\ g_{catalyst}}$ number of mol of TBHP converted at 0.5 h reaction time per gram of catalyst;

$\frac{0.014\ mol\ FW-Ti}{mol\ (Si+Ti)}$ was determined from XPS analysis (Table 3);

$\frac{0.015\ mol\ (Si+Ti)}{g_{catalyst}}$ was determined from ICP-AES analysis.

*Experimental setup for catalytic tests*

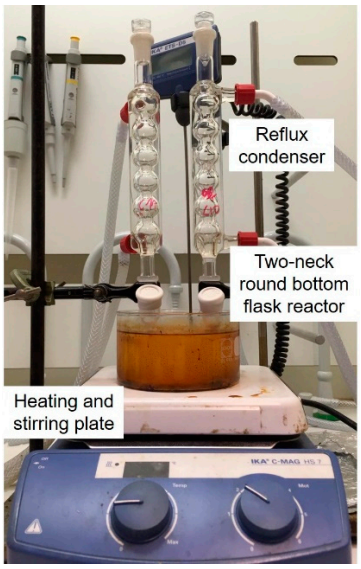


**Figure S9.** Experimental setup for catalytic tests.

## References

1. Vivian, A.; Fusaro, L.; Debecker, D.P.; Aprile, C. Mesoporous Methyl-Functionalized Sn-Silicates Generated by the Aerosol Process for the Sustainable Production of Ethyl Lactate. *ACS Sustain. Chem. Eng.* **2018**, *6*, 14095–14103, doi:10.1021/acssuschemeng.8b02623.
2. Grudzien, R.M.; Grabicka, B.E.; Jaroniec, M. Effective method for removal of polymeric template from SBA-16 silica combining extraction and temperature-controlled calcination. *J. Mater. Chem.* **2005**, *16*, 819–823, doi:10.1039/b515975j.
3. Perugachi, L.E.M.; Vivian, A.; Eloy, P.; Debecker, D.P.; Aprile, C.; Gaigneaux, E.M. Hydrophobic titania-silica mixed oxides for the catalytic epoxidation of cyclooctene. *Catal. Today* **2019**, doi:10.1016/j.cattod.2019.05.020.
4. Stakheev, A.Y.; Shpiro, E.S.; Apijok, J. XPS and XAES study of titania-silica mixed oxide system. *J. Phys. Chem.* **1993**, *97*, 5668–5672, doi:10.1021/j100123a034.
5. Vetter, S.; Schulz-Ekloff, G.; Kulawik, K.; Jaeger, N.I. On the para/ortho product ratio of phenol and anisole hydroxylation over titanium silicalite-1. Chem. Eng. Technol. **1994**, *17*, 348–353.
6. Tyablikov, I.A.; Rodionova, L.I.; Sobolev, P.D.; Ivanova, I.I. Formation of active sites in titanium-containing zeolites with MFI structure in propylene epoxidation with hydrogen peroxide. *Pet. Chem.* **2016**, *56*, 267–274, doi:10.1134/s0965544116030142.
7. Langerame, F.; Salvi, A.M.; Silletti, M.; Moretti, G. XPS characterization of a synthetic Ti-containing MFI zeolite framework: The titanosilicalites, TS-1. *Surf. Interface Anal.* **2008**, *40*, 695–699, doi:10.1002/sia.2739.
8. Yamashita, H.; Kawasaki, S.; Ichihashi, Y.; Harada, M.; Takeuchi, A.M.; Anpo, M.; Stewart, G.; Fox, M.A.; Louis, C.; Che, M. Characterization of Titanium−Silicon Binary Oxide Catalysts Prepared by the Sol−Gel Method and Their Photocatalytic Reactivity for the Liquid-Phase Oxidation of 1-Octanol. *J. Phys. Chem. B* **1998**, *102*, 5870–5875, doi:10.1021/jp981343a.
9. Hasegawa, Y.; Ayame, A. Investigation of oxidation states of titanium in titanium silicalite-1 by X-ray photoelectron spectroscopy. *Catal. Today* **2001**, *71*, 177–187, doi:10.1016/s0920-5861(01)00428-x.
10. Wagner, C.; Riggs, W.; Davis, L.; Moulder, J.; Muilenberg, G. Handbook of X-ray Photoelectron Spectroscopy; Muilenberg, G., Ed. Perkin-Elmer Corporation, Physical Electronics Division: Eden Prairie, MN, USA, 1979.
11. Smeets, V.; Boissière, C.; Sanchez, C.; Gaigneaux, E.M.; Peeters, E.; Sels, B.F.; Dusselier, M.; Debecker, D.P. Aerosol Route to TiO2–SiO2Catalysts with Tailored Pore Architecture and High Epoxidation Activity. *Chem. Mater.* **2019**, *31*, 1610–1619, doi:10.1021/acs.chemmater.8b04843.
12. Erdem, B.; Hunsicker, R.A.; Simmons, G.W.; Sudol, E.D.; Dimonie, V.L.; El-Aasser, M.S. XPS and FTIR Surface Characterization of TiO2Particles Used in Polymer Encapsulation. *Langmuir* **2001**, *17*, 2664–2669, doi:10.1021/la0015213.